AIChE

Modeling Ice Removal in Fluidized-Bed Freeze Concentration of Apple Juice

S. Nazir and M.M. Farid
Dept. of Chemical and Materials Engineering, The University of Auckland, Private Bag 92019, New Zealand

DOI 10.1002/aic.11602
Published online September 24, 2008 in Wiley InterScience (www.interscience.wiley.com).

Stable operation of fluidized-bed heat exchangers during freeze concentration is limited by the rate of ice removal from the cooling surfaces. Operation remains stable as long as the erosion rate caused by the fluidized particles is equal or greater then the ice growth rate. An empirical model has been devised to estimate the erosion rate at different operating conditions. 4 and 5 mm equilateral cylindrical particles made of stainless steel (SS304) were fluidized in the inside pipe of a vertical double pipe heat exchanger. Bed porosities of 0.94–0.76, and apple juice concentrations of 12, 16, 18, and 20 Brix were tested. The new erosion model was developed based on an analogy between erosion and heat-transfer phenomenon. Experimental values of erosion rate were obtained for different operating conditions and compared with the values estimated by the model. © 2008 American Institute of Chemical Engineers *AIChE J,* 54: 2999–3006, 2008

Keywords: fluidized-bed heat exchangers, erosion model, liquid fluidization, freeze concentration, heat transfer

Introduction

Fluidized-bed freeze concentration is a novel technique which can be applied to the freeze concentration of liquid foods. The scraped surface heat exchanger (SSHE) is the most expensive piece of equipment in conventional freeze concentration processes.[1] The high quality of concentrated fruit juice produced by freeze concentration process[2] has instigated this work to investigate the applicability of fluidized-bed freeze concentration to concentrate apple juice. This work contributes to the research underway to make freeze concentration technology acceptable to the industry. FBHE can be visualized as a vertical double pipe or a shell and tube heat exchanger with particles fluidized in the tubes. The best understanding of fluidized-bed freeze Concentration process is achieved by the knowledge of ability of fluidized particles to remove ice from the cooling surfaces. There is a maximum cooling duty that can be applied at which the growth rate of ice on cooling surface becomes equal to the rate of ice removal. Exceeding this limit will result in failure of the operation and freeze up of the fluidized-bed column. Mathematical models have been engineered for erosion in Liquid fluidized beds erosion caused by fluidized bed during freeze concentration.[1,3] In these models, the system was considered to be in particulate mode and the particle-particle interaction was considered insignificant. We believe that, with the change in hydrodynamic characteristics of the fluidized bed, the motion of the particles changes which affects the rate of erosion rate. Therefore, the effects of hydrodynamics have to be taken into account in the development of liquid fluidized-bed erosion models.

Hydrodynamics of liquid fluidized beds

Depending on bed porosity, particle and solution characteristics, liquid fluidized-bed hydrodynamics generally behave in two modes namely, particulate (or segregate) and aggregate (or bubbling). In the particulate mode, the fluidized bed is homogeneous with particles distributed uniformly throughout the bed.[4] In this mode, characteristic motion of individual

Correspondence concerning this article should be addressed to M. Farid at m.farid@auckland.ac.nz.

particle is pivotal.[3] Therefore, it is important to understand the particle's kinetic energy and the frequency with which it strikes the wall. In the aggregate mode of fluidization, particle-particle interaction exceeds a certain value and motion of groups of particles rather then individual particle becomes important. The aggregate mode is manifested by the movement of small groups of particles as individual units through the system.[5] These small groups or clusters of particles rise through the bed and burst through the surface creating a high-degree of solid and liquid mixing. Figure 1 describes these two major modes of operation in liquid fluidization.

Mode of fluidization can be identified by a simple hydrodynamic criterion developed by Gibilaro.[6] According to this criterion, aggregation in fluidized bed will occur if the following condition applies

$$Fu = \frac{u_e - u_\varepsilon}{u_e} < 0 \tag{1}$$

The dynamic wave velocity u_e can be obtained from the following equation,[7]

$$u_e = \sqrt{\frac{2.3 g d_p (1-\varepsilon)(\rho_s - \rho_l)}{\rho_s}} \tag{2}$$

The continuity wave velocity u_ε is defined by the following relationship

$$u_\varepsilon = n v_t (1-\varepsilon)\varepsilon^{n-1} \tag{3}$$

where n is the Richardson and Zaki exponent,[14] and v_t is the terminal falling velocity of particle corrected for hindering effects of tube wall.

Positive values of Fu calculated by Eq. 1 indicates particulate fluidization mode, while negative values indicate aggregate mode. Zero value of Fu indicates the conditions at which transition from particulate to aggregate takes place. It should be noted that the transition is not abrupt and takes place gradually.

Erosion modeling in liquid fluidized beds

Meijer in his work shed a considerable light on the erosion phenomenon in liquid fluidized beds, as he focused on $CaSO_4$ scale inhibition during desalination of sea water.[3] The model developed by him was based on particulate mode of fluidization and general equation proposed by him is as follows

$$E_{er} = C m_p {v_{p,x}}^2 \frac{E}{\lambda'^2} f_r \tag{4}$$

C is a constant depending on the properties of the target material, $v_{p,x}$ is the component of velocity of particle in the direction normal to the wall. Other components of velocity were neglected due the lubricating effects of liquid.[3]

The frequency of collisions per unit wall area, was further defined as the product of particle velocity and available number of particles per unit volume N

$$f_r = v_{p,x} N = \frac{6 v_{p,x}(1-\varepsilon)}{\pi d_p^3} \tag{5}$$

Every particle was supposed to be equally contributing to the collective erosion effect caused by the fluidized bed which is

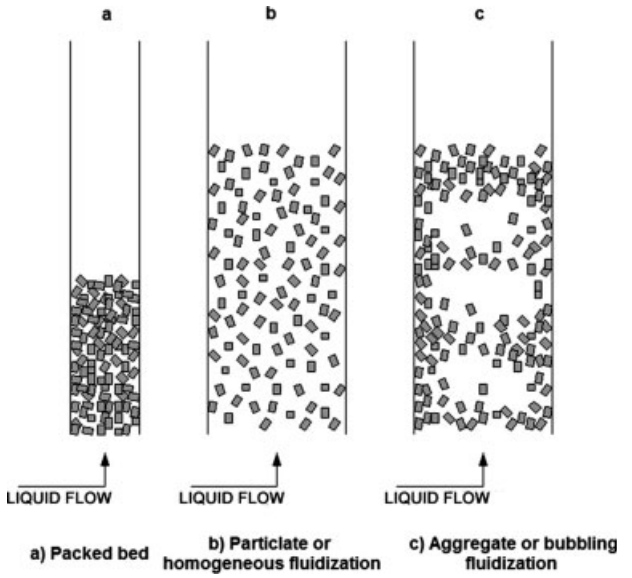

Figure 1. Hydrodynamic modes in Liquid fluidization.

the characteristic of fully particulate mode. Operating mode of fluidization in Meijer's work remained within the particulate mode as he used 23 mm ceramic balls in sea water.[3] Meijer noticed that when system went closer to bed porosity of 0.7, Eq. 4 was no longer applicable.[3] Scale of aggregation based on experimental conditions of Meijer's work indicates that fluidization turns into aggregate at this bed porosity, this is an important observation and provides a drive to furnish a different model for aggregate mode.

Habib and Farid[1] followed Meijer's assumption that the majority of collisions are in the direction normal to the wall. They pointed out that the erosion is a result of repeated collisions of particles with the walls and is not a cutting phenomenon. Therefore, they employed the modeling approach presented by Wood and Woodford,[8] which is based on the principal of fatigue erosion, developed originally for erosion in gas-fluidized beds. Following the principle presented by Hutchings[9] based on low-cycle fatigue in metals caused by the particles, final form of the equation for erosion rate was developed as shown below[1]

$$E_{er} = \frac{1.5 \gamma m_p {v_{p,x}}^3 (1-\varepsilon)}{\pi d_p^3} \tag{6}$$

where $\gamma = \frac{\beta}{N_f p}$. Where β is fraction of indented volume actually deformed in a collision, N_f is the number of impact cycles to fatigue failure, p is indentation pressure required for erosion. Eq. 6 is very similar to Meijer's erosion model (Eq. 4) with the same hydrodynamic group and a constant depending on the properties of target material.

In this study, owing to the FBHE operation falling into the aggregate mode, a new erosion model is developed and validated for ice removal from the surface of heat exchanger during freeze concentration of apple juice. This erosion model can be used to estimate the operational limits in terms of maximum cooling duty that can be applied.

Experimental setup and methods

A vertical double pipe heat exchanger was employed in this study to test fluidized-bed heat exchanger for the freeze concentration of apple juice. Details of the experimental setup has been described in a previous publication.[10] Coolant was pumped in the annular space between the inner and outer pipe in a countercurrent direction to the juice flowing upward in the inner pipe. The upward motion of the juice caused the equilateral cylindrical stainless steel particles to fluidize. Stainless steel particles, made of SS304 were manufactured commercially by cutting rods into equally sized (4, 5 mm) particles with sharp edges.

Bed porosity in fluidized bed was calculated according to the following equation

$$\varepsilon = 1 - \frac{V_p}{V_T} \tag{7}$$

V_p is the total volume occupied by the particles, and V_T is the total volume of fluidized bed. Since volume of the fluidized bed was fixed in this study, measured mass of the particles was added in order to get the desired bed porosity according to the following equation

$$\text{Mass of particles required} = V_T(1-\varepsilon)\rho_s \tag{8}$$

where ρ_s is the density of the solid particles (7,900 kg/m^3 for SS304). Once the particles were fluidized, the flow rate was adjusted to expand the fluidized bed to the whole volume and measured value of superficial velocity was recorded. Bed porosity as a function of superficial velocity was obtained by the correlation proposed by Hirata and Bulos,[11] and modified by Jamialahmadi[12] for cylindrical particles. The relationship is given as follows

$$\varepsilon = \varepsilon_{pk} + \left(1-\varepsilon_{pk}\right)\varepsilon_{RZ}^{\,7.4025+0.69\left(d_p/D\right)}\exp(7.56(1-\varepsilon_{RZ})) \tag{9}$$

ε_{PK} is the packed bed porosity and was estimated by the following equation[13] for cylindrical particles

$$\varepsilon_{pk} = \frac{0.15}{\left(\frac{D}{d_p}-1\right)} + 0.39 \quad \mathrm{D/d_p} \geq 2.033 \tag{10}$$

Richardson and Zaki bed porosity (ε_{RZ}) was calculated by the following equation[15]

$$\varepsilon_{RZ} = \left(\frac{v_s}{v_t}\right)^{1/n} \tag{11}$$

v_t is the terminal falling velocity corrected for the wall effects, and n is Richardson and Zaki exponent which may be calculated as follows[14]

$$n = \frac{2\left(2.35 + 0.175\mathrm{Re}_t^{\,0.75}\right)}{1 + 0.175\mathrm{Re}_t^{\,0.75}} \tag{12}$$

Terminal particle Reynolds number Re_t, and, hence, v_t were estimated by the empirical expression produced by Hartman[16]

$$Log_{10}\mathrm{Re}_t = P(C) + \log_{10}R(C) \tag{13}$$

where

$$P(C) = ((0.0017795C - 0.0573)C + 1.0315)C - 1.26222$$
$$R(C) = 0.99947 + 0.01853\sin(1.848C - 3.14)$$

and

$$C = \log_{10}\left[\frac{d_p^3 g\rho_l(\rho_s-\rho_l)}{{\mu_l}^2}\right]$$

Re_t is the Reynolds number at terminal falling velocity and is given by

$$\mathrm{Re}_t = \frac{v_t d_p \rho_l}{\mu_l} \tag{14}$$

The equivalent diameter, which is the diameter of a sphere of equal volume as of the particle, was used in all the calculation

$$d_p(eq) = \sqrt[3]{\frac{3}{2}d^3} \tag{15}$$

where d is the diameter of an equilateral cylindrical particle. The gross rate of heat removal from the fluidized bed was calculated from the inlet and outlet temperature of the coolant side according to the following equation

$$Q_T = m_c c_{p,c}(T_3 - T_2) \tag{16}$$

where T_3 is the coolant outlet temperature, and T_2 is the coolant inlet temperature. Although the outer surface of the heat exchanger was insulated, small amount of heat would always have been transferred from the atmosphere to the coolant. This heat transferred from the atmosphere would contribute to the total duty of the exchanger. Heat transferred from the atmosphere should be subtracted from the total duty calculated by Eq.16 in order to obtain the net rate of heat removal from the process fluid

$$Q_{net} = Q_T - Q_{atm} \tag{17}$$

where Q_{atm} is the heat gained from the atmosphere through the insulated wall of the shell of heat exchanger. Q_{atm} was calculated by considering average ambient temperature of 18°C. Thermal conductivities of 0.092 W/mK and 0.036 W/mK for PVC pipe and insulation (FR/Armaflex), respectively, were used in the calculations.

In the experiments coolant inlet temperature was varied from −3°C to −14°C depending on the juice freezing temperature (i.e., its concentration). Coolant flow was adjusted at a maximum value of 1 kg/s. Pulp free apple juice was tested in concentrations of 12, 16, 18 and 20° brix, which were prepared by diluting 70° brix apple juice concentrate. Concentrations were measured using calibrated digital refractometer under controlled temperature of 20°C. In each experiment, the feed tank was filled with 70L of juice.

Table 1. Correlations for Estimating Physical Properties of Apple Juice

Physical Property	Correlation	Eq. no.	Ref. no.	Remarks
Viscosity, μ	$\ln \mu = \frac{(0.45\,C^2 + 4.11C + 2.04 \times 10^3)}{T} + (-1.03 \times 10^{-3}C^2 + 6.44 \times 10^{-3}C - 13.8)$	22	17	C is concentration in °Brix, T is Temperature in K
Density, ρ	$\ln \rho = -(2.64 \times 10^{-6}\,C + 2.66 \times 10^{-4})T - (-4.98 \times 10^{-3}\,C + 13.8)$	23	17	C is concentration in °Brix, T is Temperature in K
Thermal Conductivity, k	$k = (0.565 + 0.0018T - 6 \times 10^{-6}T^2)(1 - 0.54X_s)$	24	18	X_s is the mass fraction of solids, T is temperature in °C
Specific Heat, C_p	$C_p = 4.187\{1 - X_s\,[0.57 - 0.0018(T - 20)]\}$	25	18	X_s is the mass fraction of solids, T is temperature in °C

Experimental value of overall heat-transfer coefficient (OHTC), U_{exp} was calculated from experimental conditions based on outside surface area of the inner pipe as follows

$$U_{\exp} = \frac{Q_{net}}{A_o \Delta T_{LMTD}} \tag{18}$$

where Q_{net} is defined in Eq. 17, A_o is the outside surface area of the inner pipe; ΔT_{LMTD} is the log mean temperature difference, and is given by

$$\Delta T_{LMTD} = \frac{\theta_h - \theta_c}{\ln \frac{\theta_h}{\theta_c}} \tag{19}$$

where θ_h is the warm-side temperature difference, T4-T1 and θ_c is the cold-side temperature difference, T3-T2.

During freezing all heat removed from the apple juice serves to generate ice. In this study it was assumed that almost all ice is generated on the walls of the heat exchanger. The growth rate of ice can be increased by increasing the cooling rate. Ice was assumed to be distributed evenly on the exchanger wall and

$$G = \frac{Q_{net}}{H_f \rho_{ice} \pi D L} \tag{20}$$

where G is ice growth rate m/s, H_f is the latent heat of fusion of ice. Juice was cooled to its freezing point, and seeding was performed. If seeding was performed after super cooling, column had a tendency to freeze up due to rapid formation of ice layer beyond the removing capability of the solid particles. Seed crystals were prepared by freezing small volume of juice and crushing the resulting ice.

In the experiments, growth rate of ice was increased by increasing the temperature difference between process fluid and circulating coolant. This was done by lowering the refrigerant inlet temperature in small steps (0.25–0.5°C), and then, the column was allowed to operate with the same cooling rate for 10–20 min. During this time interval OHTC and pressure drop through the fluidized bed were monitored. After ensuring column stability, ice growth rate was increased by lowering the refrigerant temperature further. At a certain ice growth rate, column failure occurred, which was manifested by a decrease in heat-transfer coefficient due to the buildup of ice layer of low thermal conductivity on the exchanger walls. This was also accompanied by an increase and then decrease in pressure drop across the fluidized bed. The increase in the pressure drop is due to the buildup of ice inside the column, while the decrease in pressure drop is due to particles running out of the column as a result of decrease in cross-sectional area of the column. Particles could be seen through the transparent column installed above the fluidized bed during column failure. At critically stable condition, growth rate of ice on the exchanger wall is equal to the erosion rate caused by the solid particles. If the cooling rate increases beyond this point, growth rate of ice goes beyond the ability of solid particles to remove it, and column failure or freeze up takes place. Therefore, the experimental value of erosion rate can be obtained by equating the growth rate at critically stable condition to the erosion rate. This is essentially the same procedure adopted in previous work on fluidized-bed freeze concentration of milk and NaCl solution.[1,10] Therefore, erosion rate was evaluated as follows

$$E_{er} = G_{(crit)} \tag{21}$$

Correlations given in Table 1 were used for estimating physical and thermal properties of apple juice (Table 1).

Development and validation of erosion model

Based on our discussion in the previous section, it was necessary to device an erosion model for liquid fluidized beds in aggregate mode. This model would be of considerable importance as fluidized-bed freeze concentration plants would almost always operate in aggregate mode.

Heat transfer has been extensively studied and understood in liquid fluidized beds. It was found that the increased heat-transfer coefficient in a fluidized bed was mainly due to disturbance and mixing of the fluid within the thermal boundary layer caused by the fluidized particles.[12] The fluidized particles collide repeatedly with the walls and the faster the movement the greater the heat transfer coefficient.[13] It has also been noticed that once fluidization turns into aggregate mode, changing particle size does not affect heat-transfer coefficient significantly. Whereas, particle size does have a considerable effect on heat transfer coefficient in particulate mode of fluidization.[12] The experimental results presented later in this article show that particle size has a negligible effect on erosion rate in FBHE and operation mode was aggregate. These findings encouraged us to devise an erosion model in analogy with heat transfer.

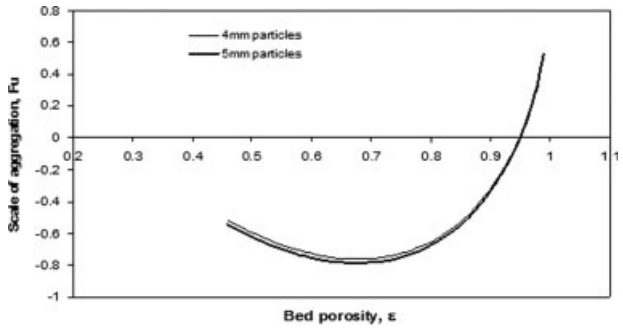

Figure 2. Calculation of scale of aggregation to predict the hydrodynamic behavior of the fluidized bed for 4 and 5 mm cylindrical particles and 12 °Brix apple juice.

Meewisse's heat-transfer model for wall-to-bed heat-transfer coefficient was found to be most suitable when compared with the wall-to-bed heat-transfer coefficients found experimentally in this work.[19] The correlation to evaluate wall-to-bed heat-transfer coefficient suggested by Meewisse is shown as follows[20]

$$Nu_h = 0.0587\mathrm{Re}_h^{0.709}\mathrm{Pr}^{0.622} \tag{26}$$

where

$$Nu_h = \frac{hd_p}{k_l}\frac{\varepsilon}{1-\varepsilon}$$

$$\mathrm{Re}_h = \frac{\rho v_s d_p}{\mu}\frac{1}{1-\varepsilon}$$

$$\mathrm{Pr} = \frac{c_p\mu}{k_l}$$

As discussed earlier, erosion phenomenon in liquid fluidized beds, can be defined analogous to heat transfer. A new parameter, introduced in this article, termed "*Cleaning Ability Coefficient, C_c*" may be defined by dividing the heat-transfer coefficient from Eq. 26 by the product of liquid density and its heat capacity ($\rho_l\, C_P$)

$$C_c = \frac{h}{\rho_l C_{p,l}} = 0.0587\left(\frac{\rho v_s d_p}{\mu}\frac{1}{1-\varepsilon}\right)^{0.709}\left(\frac{C_{p,l}\mu}{k_l}\right)^{0.622}\left(\frac{k_l(1-\varepsilon)}{d_p\varepsilon\rho_l C_{p,l}}\right) \tag{27}$$

The units of C_c is m/s, and, hence, it describes the ability of fluidized bed to remove the ice layer generated on the surface. Erosion rate also depends on the properties of the target material, therefore, the erosion rate can be defined as,

$$E_{er} = \gamma'\, C_c \tag{28}$$

where γ' is a dimensionless constant for the target ice and it represents the ease with which ice can be removed. As the nature of ice is expected to change with concentration and type of solution,[1,21] values of γ' are also expected to vary with the change in solution concentration. Values of γ' for different solutions and concentrations should be determined experimentally. Therefore, the final form of equation for the erosion rate becomes

$$E_{er}(m/s) = 0.0587\gamma'\frac{v_s^{0.709}k_l^{0.378}}{\rho_l^{0.291}\mu^{0.087}C_{p,l}^{0.378}d_p^{0.291}}\frac{(1-\varepsilon)^{0.291}}{\varepsilon} \tag{29}$$

This erosion model is only applicable to aggregate mode in liquid fluidized beds. This model also does not consider the angle of impact, and frequency of impact like in the models discussed previously, but these parameters are inherently included through their effect on the heat transfer, which the model is based on.

Hydrodynamics

It can be seen from Figure 2 that scale of aggregation Fu (calculated according to Eqs. 1–3) became negative at a bed porosity of 0.94 for both 4 and 5 mm particles, suggesting that operating conditions in this work fall in aggregate mode. After observing the same trend for other solution concentrations, it can be said that a change in solution concentration does not change the scale of aggregation significantly.

Experimental values of erosion rate

Measured erosion rates were obtained using the methodology presented in the previous section, employing Eqs. 20 and 21, for 12 Brix apple juice, and are shown in Figure 3. Bed porosity was calculated using Eqs. 9–15. It can be seen from Figure 3 that the erosion rate generally increases with decrease in bed porosity. This observation is in line with the experimental results found by Habib and Farid on fluidized-bed freeze concentration of milk and brine.[1,10] This increase in erosion rate is attributed to the increase in the number of particles, which increases the number of collisions per unit area of the column.

It is important to note here that the decrease in bed porosity also causes the superficial velocity of the liquid to decrease, which in turn tends to reduce the aggressiveness of the fluidized bed. Therefore, the increase in the number of particles is contributing more then the decrease in superficial velocity to this change in erosion rate.

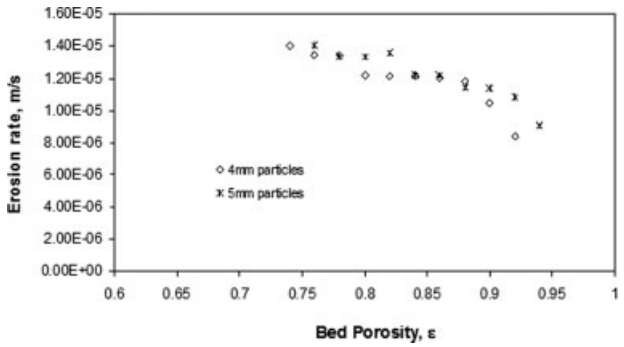

Figure 3. Variation of experimental values of erosion rate with particle size and bed porosity using 12° Brix apple juice.

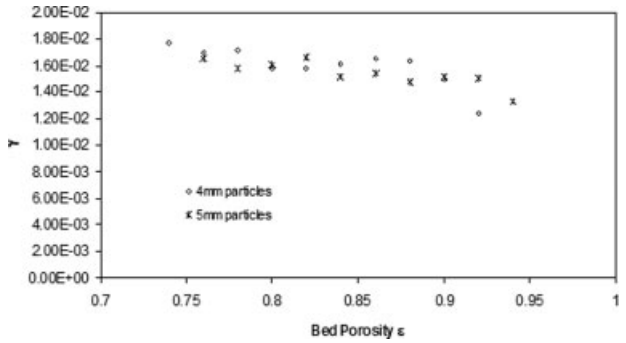

Figure 4. Values of γ' at different bed porosities according to Eq. 29 for 4 and 5 mm particles, and 12 Brix apple juice.

It is evident from Figure 3 that erosion rate changes sharply in the region of higher bed porosities (greater then 0.92), and this change becomes less pronounced with further decrease in bed porosity. This is due to the change in fluidized-bed hydrodynamics with bed porosity. From Figure 2 it can be seen that for both 4 and 5 mm particles, the fluidized bed turns into aggregate mode at bed porosity of around 0.94. Due to gradual transition between the two modes, the system happens to be in a partial aggregate state between bed porosities of 0.9 and 0.94. The increase of particle-particle collisions as the system advances into aggregate mode may explain the smaller change in erosion rate in the fully aggregate mode as manifested in Figure 3.

It can also be observed from Figure 3 that particle size has only small effect on the erosion rate. Erosion rate for 5 mm particles is only slightly higher then that for 4 mm at some bed porosities. This observation is the one, which lead to the development of the new model presented in this work. Previously, Habib and Farid[1] found that the erosion rate caused by the 4 mm particles was significantly less then 5mm particles for both milk and brine. The effect was probably due to the fact that the 4 mm particles used in their work were not as sharp as those used in this work.

We expect that the effect of hydrodynamics on heat-transfer phenomenon would be similar to its effect on the erosive ability of the particles, since both are related to what happen at the wall of the column. The movement of particles in aggregate mode in the form of clusters overshadows the effect of particle size caused by different superficial velocities. Therefore, it maybe concluded that when a fluidized bed enters aggregate mode, the effect of particle size on erosion also becomes smaller.

Evaluation of experimental values of γ'

As discussed earlier γ', in Eq. 29 is a constant depending on the nature of ice formed, which in turn is a function of type and concentration of the solution to be concentrated. Therefore, validity of the erosion model has been confirmed by obtaining experimental values of γ' for different concentrations, bed porosities and particle sizes. Obtaining a constant value of γ' for a specific concentration and type of solution is a criterion for suitability of our erosion model.

Table 2. Average Values of γ' for Different Juice Concentrations

Juice concentration, Brix	Average γ', 4 mm	Average γ', 5 mm	Average γ'
12	1.64E-02	1.57E-02	1.60E-02
16	2.14E-02	2.11E-02	2.13E-02
18	2.34E-02	2.42E-02	2.38E-02
20	2.28E-02	2.61E-02	2.44E-02

It is clear from Figure 4 that values of γ' remained constant over most of the range of bed porosities and for both particle sizes tested. There is a variation in values in γ' the region of high-bed porosity. Beyond bed porosity of 0.9, particulate fluidization dominates giving rise to increased impact of particle size on the erosion rate (phenomenon discussed in details in the previous section). γ' values change with solution concentration, therefore, experiments performed with higher concentration of apple juice yielded different values. Final values of γ' were obtained by taking averages over a range of bed porosities and two particle sizes. Values of γ' for bed porosities above 0.9 were neglected since fluidization follows different mechanisms as described earlier. Summery of these results is shown in Table 2 and plotted in Figure 5.

It can be seen that values of γ' vary linearly with juice concentration. This result conforms to the experimental results on milk and brine.[1] It was discussed earlier that represents the ease with which ice can be removed. Therefore, from this result it can be inferred that with the increase in solution concentration, ease of ice removal increases so does the erosion rate. Habib and Farid[1] explained this increase in γ', with concentration to be a result of a decrease in γ' strength of ice, with the increase in solution concentration. Meewisse[21] reported similar results during his work on ice slurry generation using fluidized bed, and attributed this effect to the reduced crystal growth rate due to increased solution concentration.

Modeling results

Erosion rate model (Eq. 29) was used to calculate the erosion rates and compared them with experimentally measured values (Eqs. 20 and 21) as shown in Figure 6a and b. Experimental values of superficial velocities were used in the calculation of erosion rate by Eq. 29. The linear relationship between γ' and juice concentration (Figure 5) was used for calculating γ'.

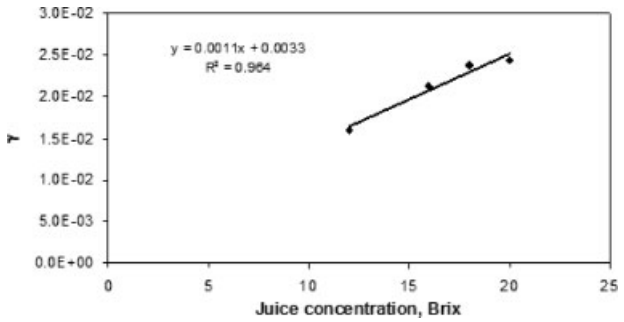

Figure 5. Variation of γ' with solution concentration.

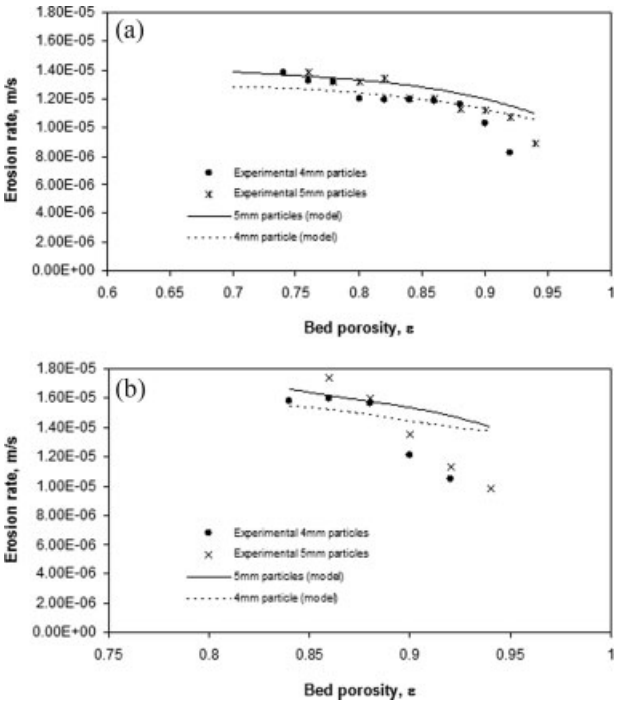

Figure 6. (a) Comparison of calculated and experimental values of erosion rate for 4 and 5 mm particles, and 12° Brix apple juice; (b) comparison of calculated and experimental values of erosion rate for 4 and 5 mm particles, and 16° Brix apple juice.

It can be observed in Figure 6a and b that the model predicts a slightly higher erosion rate for 5 mm than 4 mm particles at higher bed porosities, which is also evident from the experimental measurements. Aggregate behavior in the bed diminishes the difference in the erosion rates between two particle sizes. Because of particulate behavior in the fluidized bed, model does not conform well to the experimental results at higher-bed porosity range (see Figure 6b).

For juice concentrations of 18 and 20°Brix, experiments at bed porosities lower than 0.88 could not be performed due to limited cooling duty performed by the chiller. The small number of experiments at higher concentration was not sufficient to yield very meaningful erosion curves, but was sufficient to approximate the values of γ'. Further experimental work is required using a more efficient cooling system.

It can be seen that the erosion model conforms to the experimental results well. Erosion rate drops at higher- and lower-bed porosities. At higher-bed porosity erosion rate drops due to the less number of particles in the bed, while at lower-bed porosity, the drop in erosion rate is due to restriction in the movement of particles caused by the presence of large number of other particles.

Conclusions

Experiments show that it is possible to carry out freeze concentration of fruit juices in fluidized-bed heat exchanger. However, the fact that such a process can be stable (the condition in which the rate of ice removal is higher or equal to the rate of ice formation) at only specific operating conditions, required the development of a model to predict these stable conditions. Experimental results have shown that particle size had only a small effect on erosion rate of the ice formed in the process. Analogy between heat transfer and erosion phenomenon has led to the development of a new erosion model. This erosion model predicts stable operating limits for the fluidized bed at different bed porosities, particle sizes and concentrations of apple juice. The model predicts the experimental values well at bed porosities lower than 0.9, due to the fact that the fluidized bed operates at aggregate mode. Impact of particle shape has not been studied in this work, therefore, there is a need for more work in this avenue to incorporate the effect of particle shape.

The model developed here can be applied to media other than apple juice, provided, values of are obtained experimentally for use in the model. This study does help in improving the understanding of freeze concentration operation in liquid fluidized beds.

Notation

A = area, m^2
C_p = specific heat capacity, J kg^{-1} $°C^{-1}$
d_p = equivalent particle diameter, m
D = fluidized-bed diameter, m
E = elasticity modulus, Nm^{-2}
E_{er} = erosion rate, m sec^{-1}
f_r = frequency of impact per unit area, number $sec^{-1}m^{-2}$
g = acceleration due to gravity = 9.81 $msec^{-2}$
G = ice growth rate, $msec^{-1}$
h = wall-to-bed heat-transfer coefficient, Wm^{-2} $°C^{-1}$
Fu = scale of aggregation.
k = thermal conductivity, Wm^{-1} $°C^{-1}$
L = length, m
m = mass, kg
N = number of particles per unit volume, m^{-3}
Nu_p = particle Nusselt number
Nu_h = hydraulic Nusselt number
Q = heat duty, W
Re_h = hydraulic Reynolds number
r = radius, m
T = temperature, °C
v_s = superficial velocity
V_t = total volume of fluidized bed, m^3
W_{er} = eroded volume per impact, m^3

Greek letters

ε = bed porosity or void fraction
λ' = yield stress, Nm^{-2}
ϕ = angle of impact
μ = dynamic viscosity, Pas
ρ = density, kgm^{-3}

Subscripts

atm = atmosphere
c = coolant
h = hydraulic
i = ice slurry
in = inside
l = liquid
o = outside
P = particles
s = solid particles
T = total
exp = experimental
x = direction normal to the wall

Literature Cited

1. Habib BA, Farid MM. *Fluidized bed freeze concentration.* Auckland: Chemical & Materials Engineering, University of Auckland; 2006. Phd Thesis.
2. Thijssen HAC, Middelberg LRWA. Fundamentals in fruit juice concentration. Located at: *Refrigeration science and technology, concentration and purification by freezing*. Delft, Netherlands; 1966.
3. Meijer JAM. *Inhibition of calcium sulfate scale by a fluidized bed.* 1984. PhD Thesis, University of Delft, The Netherlands.
4. Couderc JP. Incipient fluidization and particulate systems. In: Davidson JF CR, Harrison D, ed. *Fluidization*. 2nd ed. London: Academic Press; 1985:1–46.
5. Mickley S, Fairbanks DF. Mechanism of heat transfer to fluidized beds. *AIChE J*. 1955;1:374–384.
6. Gibilaro GL, Hossain I, Foscolo PU. Aggregative behaviour of Liquid Fluidized beds. *Can J Chem Eng*. 1986;64:931–938.
7. Foscolo PU, Gibilaro LG. A fully predictive criterion for the transition between particulate and aggregate fluidization. *Chem Eng Sci*. 1984;19(1667–1675).
8. Wood RT, Woodford DA. Effect of particle size and hardness on material erosion in fluidized beds. Paper presented at: *Proceedings of the 6th International Conference on Erosion by Liquid and Solid Impact,* 1983; Cambridge, U.K.
9. Hutchings IM. Some comments on the theoretical treatment of erosive particle impacts. Paper presented at: *Proceedings of 5th International Conference on Erosion by Solid and Liquid Impact,* 1979; Cambridge, England.
10. Habib BA, Farid MM. Heat transfer and operating conditions for freeze concentration in a liquid-solid fluidized bed heat exchanger. *Chem Eng Process*. 2006/8 2006;45(8):698–710.
11. Hirata A, Bulos FB. Predicting bed voidage in solid-liquid fluidization. *J Chem Eng Jap*. Oct 1990;23(5):599–604.
12. Jamialahmadi M, Muller-Steinhagen H. Hydrodynamics and heat transfer of liquid fluidized bed systems. *Chem Eng Commun*. 2000; 179:35–79.
13. Aghajani M, Muller-Steinhagen H, Jamialahmadi M. New design equations for liquid/solid fluidized bed heat exchangers. *Int J Heat Mass Transf*. 2005;48(2):317–329.
14. Rowe PN. A convenient empirical equation for the estimation of the Richardson and Zaki exponent. *Chem Eng Sci*. 1987;42:2795–2796.
15. Richardson JF, Zaki WN. Sedimentation and Fluidization: Part 1. *Trans Inst Chem Eng*. 1954;32:35–55.
16. Hartman M, Havlin V, Trnka O, Carsky M. Predicting the free fall velocities of spheres. *Chem Eng Sci*. 1989;47(8):3162–3166.
17. Tagawa A, Muramatsu Y, Kitamura Y, Tanaka C. A new experimental equation for viscosity of liquid food involving concentration dependence. *Nippon Shokuhan Kogyo Gakkaishi/J Jap Soc Food Sci Technol*. 1997;44(1):69.
18. Nagy S, Chen CS, Shaw PE. *Fruit Juice Processing technology*. Auburndale, Florida: Agscience, Inc; 1993.
19. Nazir S, Farid MM. *Fluidized bed freeze concentration of Fruit Juices [(Unpublished)].* Auckland: Chemical and Material Engineering, University of Auckland; 2006. MEng Thesis.
20. Meewisse JW, Infante Ferreira CA. Validation of the use of heat transfer models in liquid/solid fluidized beds for ice slurry generation. *Int J Heat Mass Transf*. 2003;46(19):3683–3695.
21. Meewisse JW. *Fluidized bed ice slurry generator for enhanced secondary cooling systems.* The Netherlands: Engineering Thermodynamics, Delft University of Technology; 2004. PhD thesis.

Manuscript received Apr. 2, 2007, and revision received May 20, 2008.